Structural Engineering and Mechanics, Vol. 3, No. 1 (1995) 11-23
DOI: http://dx.doi.org/10.12989/sem.1995.3.1.011

Three-dimensional analysis of stress and strain transmission through line joints of spatial linkage of plates

G. Rosenhouse‡, A. Rutenberg‡ and Y. R. Goldfarb†

Faculty of Civil Engineering, Technion, Israel Institute of Technology, Technion City, Haifa 32000, Israel

Abstract. The examined model consists of two substructures linked by a right angle rigid line joint. One element is a wall loaded externally along its upper edge by an uneven vertical load. The other element, defined as a plate, is not loaded. Stresses and displacements in the vicinity of the joint are analysed, considering the lateral distribution which leads to three-dimensional effects. The proposed solution combines classical approach with numerical means, using appropriate stress distribution polynomial functions along the joint. Space structure constructions supply cases of interest.

Key words: joints; columns; walls; beams plates; deflection and stress analysis; finite elements; 3-D analysis.

1. Introduction

The effect of the joint on the response of a whole structure is due to its coupling property, because of its responsibility for transmission of stresses from the element loaded by external forces into the other parts of the structure. A careful study of the coupling caused by the joint shows on many occasions that two-dimensional analysis of the stress transmission may not suffice (Perry, B., *et al.* 1992). The need for a careful examination of the state of stress and displacement in the vicinity of the junction is due to several reasons, such as stress concentration and local elastic field at the joint, as well as decrease of loaded units displacements due to the influence of neighbouring elements. Specifically, a three-dimensional definition of stress and displacement fields in the vicinity of a rigid line joint of a coupled "plate/wall system" is discussed here, including an issue, which is not often addressed-namely the effect of restraint of plates on the stresses in the wall. Such joints, where response is clearly three-dimensional are typical to space structures, and some elementary configurations of them are shown in Fig. 1. The investigation presented here focuses on the complicated contribution of the joint to the transmission of strain energy from the loaded element to its neighbours, where the geometry and mechanical properties of the relevant elements play an important role. Classical elastic solutions practically do not exist for such cases, and the possible and common way to perform such an analysis is by numerical techniques, as was done for example in Perry, B., *et al.* 1992. These methods have now reached a level and reliability which enable a fast stress analysis of systems with complicated boundary conditions and loading distributions, having output schemes characterized by high resolution graphics. However, a different approach, where numerical analysis also takes

† Scientist/Engineer
‡ Professor

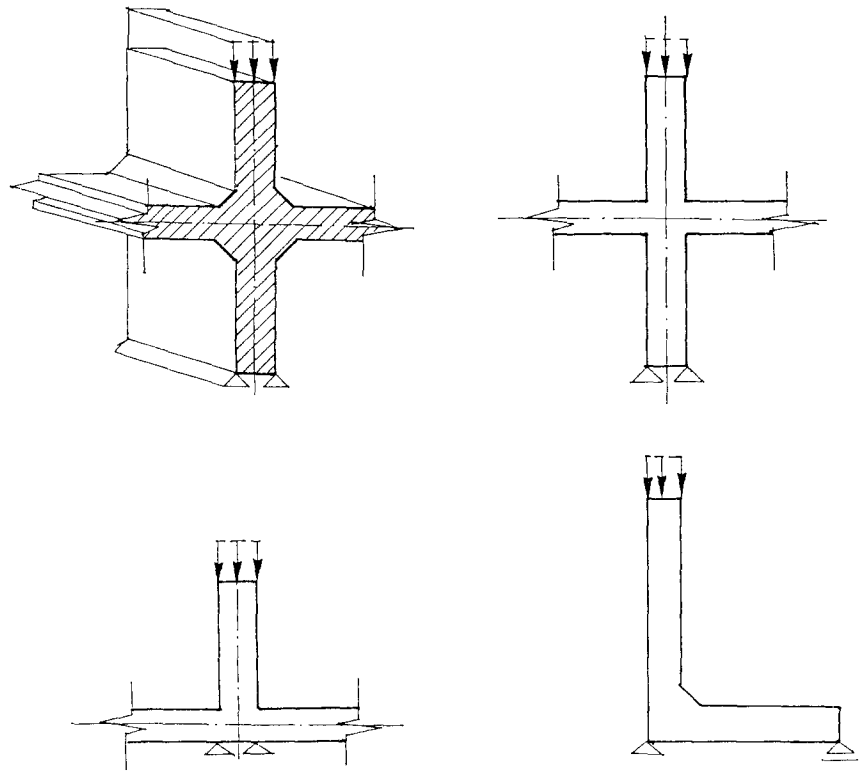

Fig. 1 Elementary structural junctions.

advantage of classical elasticity may be quite useful in finding better interpolation or distribution functions along the joints, as shown in the present work. Consequently, results obtained by the classical 2-D analysis for a specific case are used here in combination with the finite element technique for a 3-D analysis of the effect of joints between plane panels.

2. 3-D analysis of plate/wall joint under parabolic load distribution

The common assumption of uniformly distributed loads over walls in space structures may lead to the application of 2-D models. However, the existence of bending moments, shear forces, uneven distribution of vertical forces and others effects may cause lateral variations in stress and displacement distributions within the structural elements. The problem becomes more complicated in cases where the loaded unit is connected to other components of the structure, leading to an additional redistribution along the line of the joint. Last particular aspect of the problem, which means the stresses in slabs due to restraints of vertical and horizontal stresses in the walls and the lowering of wall displacements due to presence of slabs has not been addressed in literature. This consequence requires a 3-D analysis even for systems combining 2-D plane elements fixed at right angles. The present study uses a model of a "wall/plate" cross joint, where the wall is loaded along its upper edge by a normal stress of a parabolic distribution -in order to demonstrate the significance of the 3-D model, and to interpret the physical meaning of the resulting stress and displacement fields. In this context, the solution illustrated here applies

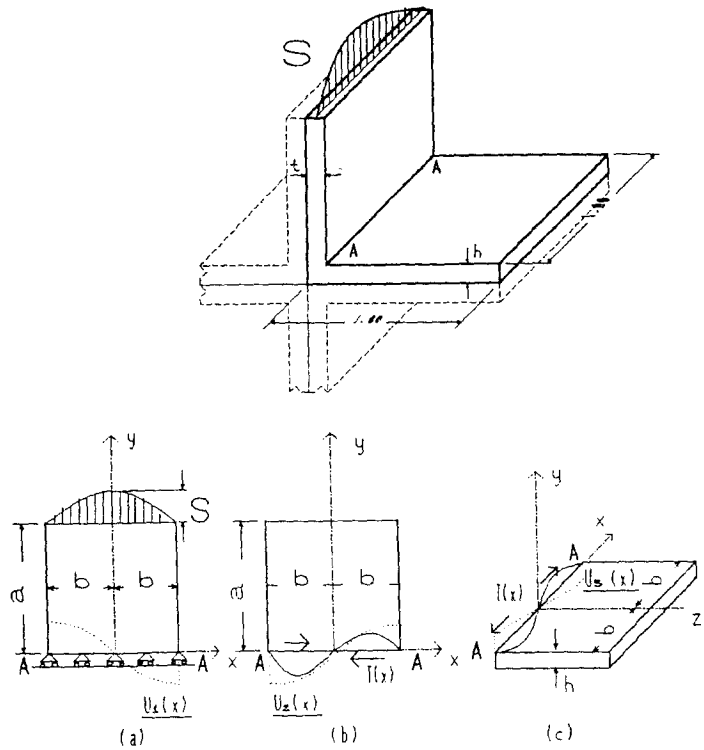

Fig. 2 A wall-plate system under a load of parabolic distribution.

a novel approach of combining numerical techniques with the theory of classical elasticity (see Appendix), which has the merit of solving the three dimensional problem expressing the compatibility between the elements by an algebraic expression.

2.1. General principles

A scheme of the system to be analyzed is shown in Fig. 2, where definition of stress in both plate and wall is sought under a variety of loading alternatives.

It should be noted that in cases of system symmetry only one quarter needs to be examined (Fig. 2), and all further descriptions are given for this quarter. The coupling caused by the rigid joint creates a redistribution of stress between the plate and the wall, which can be defined by compatibility and equilibrium along the joint.

The problem may be solved in the following four stages:

(1) Definition of a shape function for the longitudinal displacements $U_1(x)$ along the line A--A, while the plate is not yet linked to the wall. Fig. 2(a).

(2) The mutual force $T(x)$ along the joint yields there displacements $U_2(x)$, identical to those of the parabolic loading. Fig. 2(b).

(3) At this stage, the shape of the plate's displacement function $U_3(x)$ caused by $T(x)$ along A--A, is sought. In order to ensure continuity along the joint it is necessary that this shape function will be identical to those of $U_1(x)$ and $U_2(x)$. Fig. 2(c).

(4) The following compatibility condition:

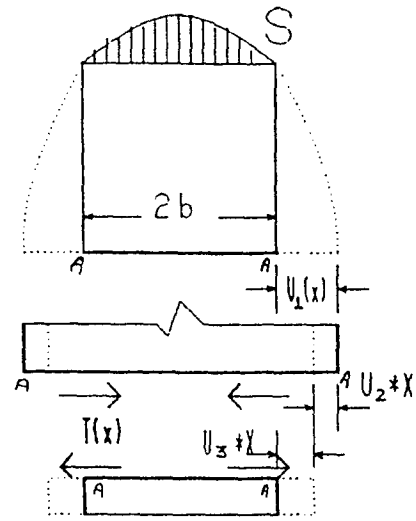

Fig. 3 The final displacements at the joint between the wall and the plate.

$$U_1(x)-U_2(x)\times X=U_3(x)\times X=U(x) \tag{1}$$

leads to stress distribution along the joint $A-A$. X is the unknown proportionality constant. The combination of the various displacements and stress distributions along the joint line are depicted in Fig. 2 and 3.

2.2. Solution

2.2.1. Definition of $U_1(x)$ for a parabolic load distribution:

$U_1(x)$ is obtained by integration of the strain ε_x:

$$U_1(x)=\int_0^x \varepsilon_x dx \tag{2}$$

The solution of the problem illustrated in Fig. 2. yields:

$$\sigma_x=\frac{\partial^2\phi}{\partial y^2}=4\alpha_1[3y^2-a^2][x^2-b^2]^2 \tag{3}$$

and along $y=0$:

$$\sigma_x=-4\alpha_1\ a^2[x^2-b^2]^2 \tag{4}$$

For comparison with results available in the literature, $\nu=0$ was assumed for Poisson ratio, although other values may also be used. Hence:

$$\varepsilon_x=\frac{\sigma_x}{E}=-\frac{4\alpha_1}{E}\ a^2[x^2-b^2]^2 \tag{5}$$

and integration yields:

$$U_{1x}=-\frac{4\alpha_1}{E}\ a^2\left[\frac{x^5}{5}-\frac{2}{3}b^2x^3+b^4x\right] \tag{6}$$

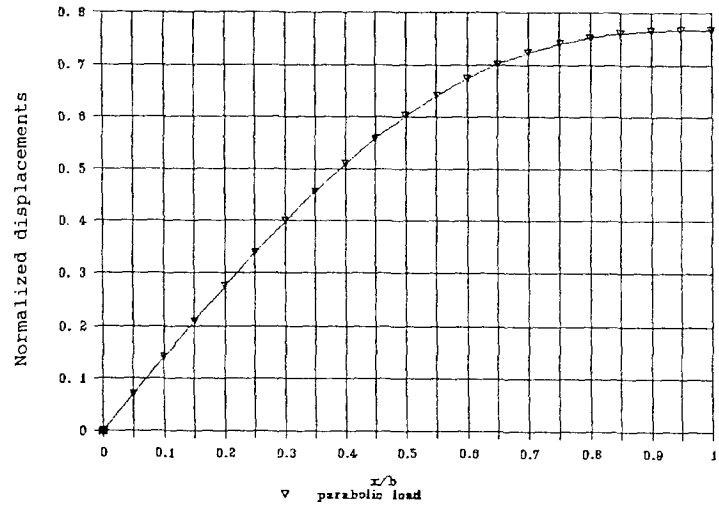

Fig. 4 Normalized $U_1(x)$ as a function of a parabolic load distribution.

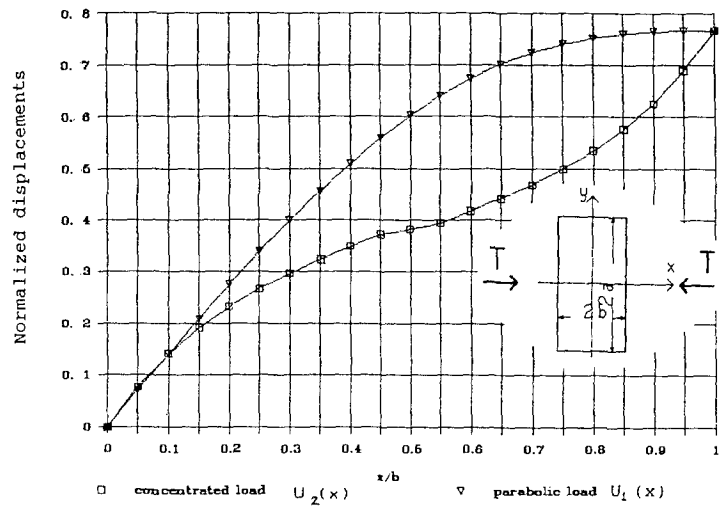

Fig. 5 Normalized $U_1(x)$ and $U_2(x)$ of point forces.

This is a polynomial of the fifth order, with the maximum displacement at $x=b$:

$$U_{1x=b}=2.133\frac{\alpha_1}{E}a^2b^5 \tag{7}$$

The shape function of $U_2(x)$ is given in Fig. 4.

2.2.2. $T(x)$ and the resulting solution for the displacement $U_2(x)$

Care should be taken in choosing $T(x)$ in order to ensure compatibility along the joint. For example, assuming $T(x)$ as point forces at the ends of the joint will not lead to compatibility, as may be observed from Fig. 5. Hence, a better choice of the coupling force $T(x)$ between the wall and the plate should be sought, satisfying the conditions:

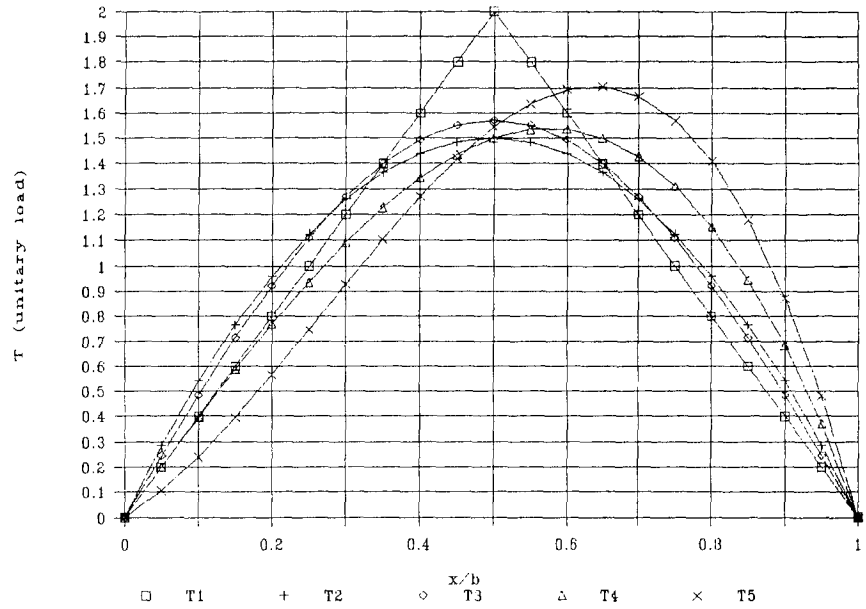

Fig. 6 A variety of chosen functions for the tangential stress $T(x)$.

(1) Continuity at $0<x<b$.
(2) Anti-symmetric distribution of $T(x)$.
(3) Boundary conditions:
T (at $x=0$)$=0$ for symmetry,
T (at $x=b$)$=0$ following Cauchy theorem.
(4) Since only the shape function of $T(x)$ is of interest, its resultant will be taken as unity. Hence $T(x)$ is defined as the stress distribution due to a unit force along half the joint length: $0<x<b$, or:

$$\int_0^b T_i(x)dx=1 \tag{8}$$

Also for convenience, $b=1.0$.
Several possibilities for the distribution of $T(x)$ were considered:
(1) Linear distribution: $T_1(x)=4x$; $0\le x\le 0.5$
$T_1(x)=4(1-x)$; $0.5\le x\le 1.0$
(2) Parabolic distribution: $T_2(x)=6x(1-x)$
(3) Sinusoidal distribution: $T_3(x)=(\pi/2)\sin(\pi x)$
(4) Third order distribution (I): $T_4(x)=4x(1-x^2)$
(5) Third order distribution (II): $T_5(x)=-8.78x^3+7x^2+1.78x$
These possibilities are shown in Fig. 6.

The displacements $U_2(x)$ and $U_1(x)$ for a parabolic load distribution are compared in Fig. 7 and the error estimate is given in Fig. 8. It is clearly observed that the best shape is a result of the choice of $T_5(x)$, with an error up to 10%. Consequently, the function chosen for $T(x)$ is $T_5(x)$.

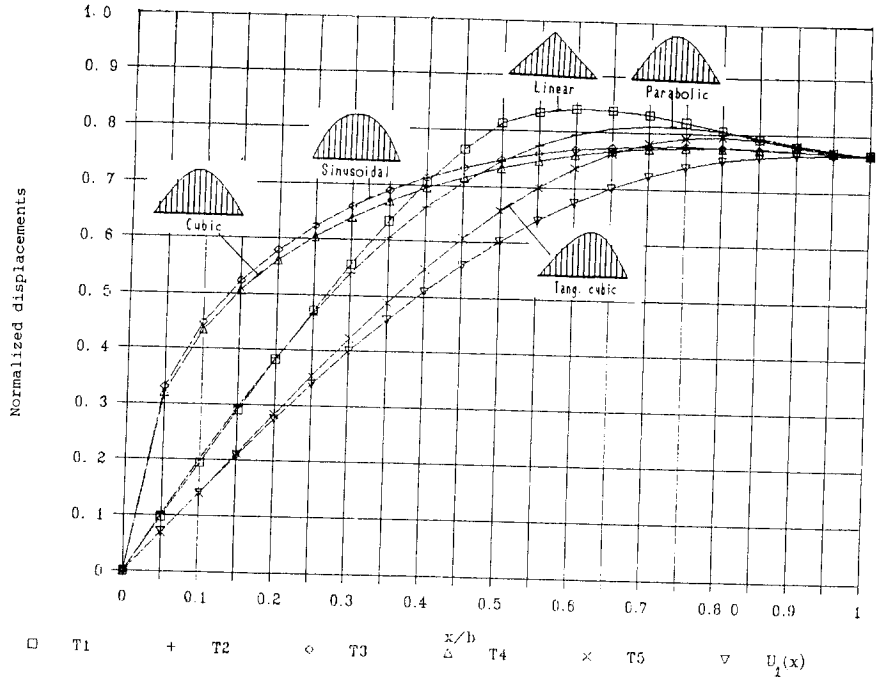

Fig. 7 Normalized displacements due to a variety of $T(x)$ and external parabolic load distributions.

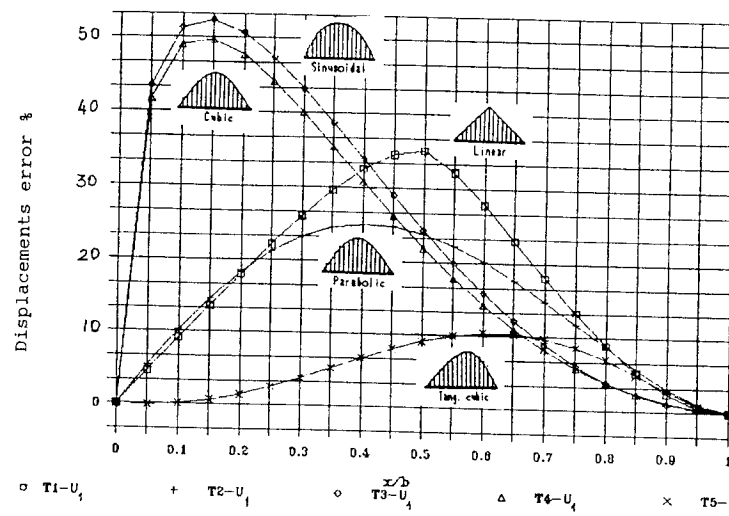

Fig. 8 Normalized absolute value of error estimate due to the choice of $T(x)$.

2.2.3. *Shape of the displacement function $U_3(x)$ at the plate due to $T(x)$*

Now, the plate displacements are examined for $T_5(x)$. The analysis is done by applying the Finite Element method, with the grid as shown in Fig. 9. The results are presented in Fig. 10 for the three lines along the joint. The solid line in that figure represents the average of the three. The resulting values lead to similar shapes for $U_1(x)$, $U_2(x)$ and $U_3(x)$, with the following maximum values at $x=b$:

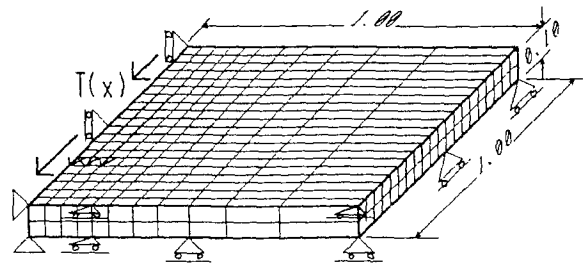

Fig. 9 F. E. grid for the plate.

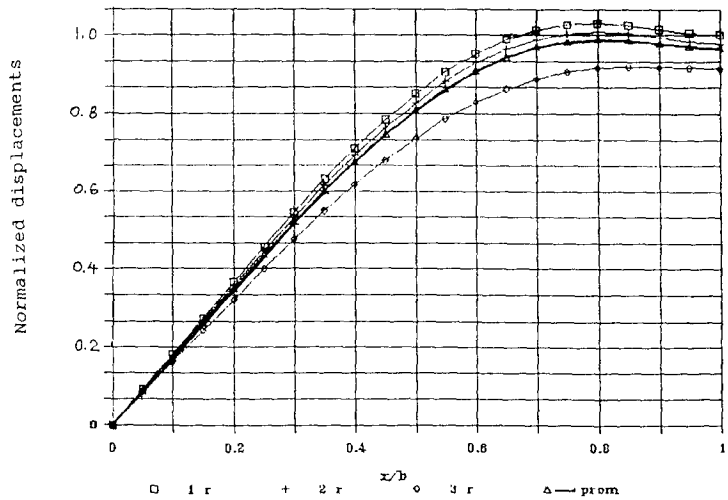

Fig. 10 Normalized displacements of the plate along the joint due to $T_5(x)$.

$$U_{1(x=b)}=0.0766,\ U_{2(x=b)}=15.418,\ U_{1(x=b)}=14.449$$

Normalizing all displacements in accordance with the value of $U_1(x)$ at $x=b$, yields the functions and the difference between them as shown in Fig. 11. Now, the proportionality coefficient x is calculated using Eq. (1), which yields: $0.0766-15.418x=14.449x$; $x=0.00256$, and the final displacement at $x=b$ is calculated as follows:

$$U=U_{1(x=b)}-U_{2(x=b)}\times X$$

$$U=0.0766-0.00256\times 15.418=0.0371,$$

which is shown in Fig. 12. Knowing $T(x)$ permits us to make a separate analysis of the stress distribution for each of the two elements of the system.

3. Conclusions

The present work illustrates an original analysis of spatial plate/wall system. Such analyses are rare since 2-D approximations are much easier. However, 3-D analysis is unavoidable when loading and boundary conditions dictate a non uniform lateral stress distribution. Such an analysis

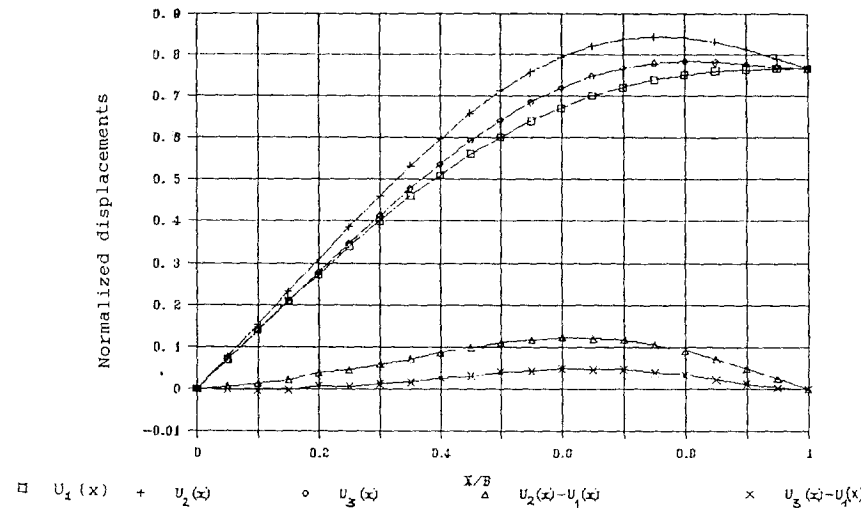

Fig. 11 Normalized displacements along the joint between the plate and the wall and the difference between them.

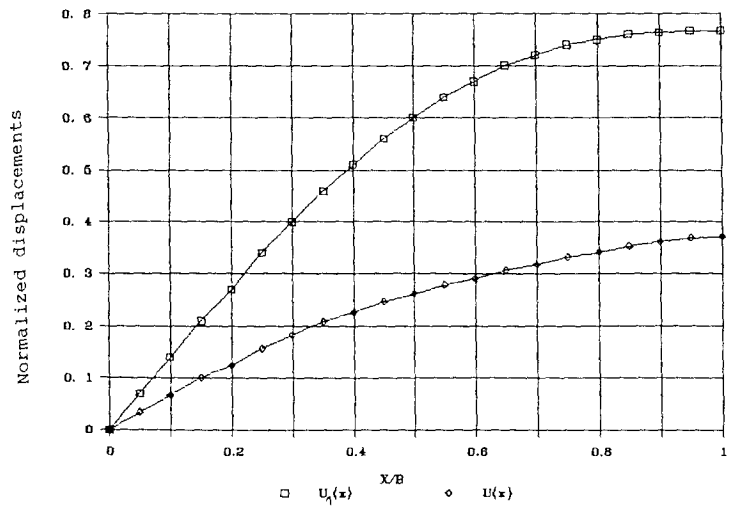

Fig. 12 Normalized final displacement $U(x)$ and $U_1(x)$.

was done for a specific case in order to find the lateral effect of the joint between the wall and the plate, taking special care about compatibility and equilibrium along the joint. Force and displacement matching resulted in a very exact solution.

Consequences of the analysis are:

(1) For the parabolic stress distribution over the wall the approximation of $T(x)$ is a polynomial of the third order, the shape of which is identical to the shape of the shear stresses along the joint for a rigidly fixed wall.

(2) The displacement function $U(x)$ is approximated by a polynomial of order five.

(3) The resulting displacement values in the plate due to $T(x)$ and in the wall, using $E=1$ and $\nu=0$, are practically the same, which means that the plate and the wall have about the same rigidity, as is to be expected.

(4) Substituting the solution in Eq. (1) shows that the differences between $U_1(x)$ and $U(x)$ are large-up to 50% (Fig. 12). Hence, the influence of the plate as a substructure should not be ignored, and the wall considered as elastically supported.

References

Perry, B., Bar-Yosef, P. and Rosenhouse, G. (1990), "On the generation and application of a new membrane and bending hybrid stress elements for analysing folded plate structures, *Proceedings of the Second World Congress of Computational Mechanics (WCCM)*, Stuttgart, **1**, 577-581.

Perry, B., Bar-Yosef, P. and Rosenhouse, G. (1992), "Rectangular hybrid shell element for analysing folded plate structures", *Computers and Structures*, **44**(1,2), 177-185.

Timoshenko, S. P. and Goodier, J. N. (1987), *Theory of Elasticity*, McGraw-Hill, New York.

Appendix

The use of classical elasticity in analysis of two-dimensional elements

1. The parabolic distribution

As an introduction to the solution of the 3-D problem, a 2-D panel loaded at its edge is examined. The example, which is illustrated in Fig. 13 (Timoshenko, S. P. and Goodier, J. N. 1987), consists of a panel loaded along its upper edge by an exact stress of a parabolic distribution. The boundary conditions of the problem are specified as follows:

$$y=\mp a\begin{cases}\sigma_y=-S\left[1-\dfrac{x^2}{b^2}\right]\\ \tau_{xy}=0\end{cases}\qquad x=\mp b\begin{cases}\sigma_x=0\\ \tau_{xy}=0\end{cases} \tag{9}$$

For, $\phi=\phi_0+\alpha_1\phi_1+\alpha_2\phi_2+\alpha_3\phi_3\cdots\cdots$, with:

$$\phi_0=\frac{1}{2}Sx^2\left[1-\frac{x^2}{6b^2}\right]$$

these boundary conditions are satisfied by:

$$\sigma_x=\frac{\partial^2\phi_0}{\partial y^2}=0$$

$$\sigma_y=\frac{\partial^2\phi_0}{\partial x^2}=S\left[1-\frac{x^2}{b^2}\right] \tag{10}$$

Assuming for Airy's function the solution:

$$\phi=\phi_0+\alpha_1\phi_1 \tag{11}$$

leads to:

$$\phi=\frac{1}{2}Sx^2\left[1-\frac{x^2}{6b^2}\right]+[x^2+b^2]^2[y^2-a^2]^2\alpha_1$$

Energy considerations lead to (Timoshenko, S. P. and Goodier, J. N. 1987):

$$\alpha_1=\frac{\dfrac{S}{a^2b^4}}{\dfrac{64}{7}\dfrac{a^2}{b^2}+\dfrac{256}{49}+\dfrac{64}{7}\dfrac{a^2}{b^2}} \tag{12}$$

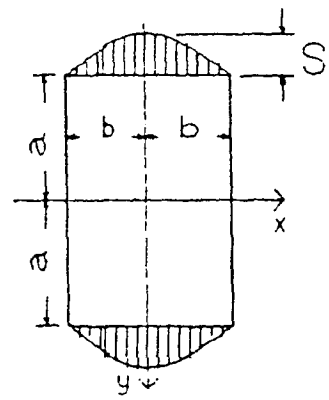

Fig. 13 A panel loaded by an edge tranction of a parabolic distribution.

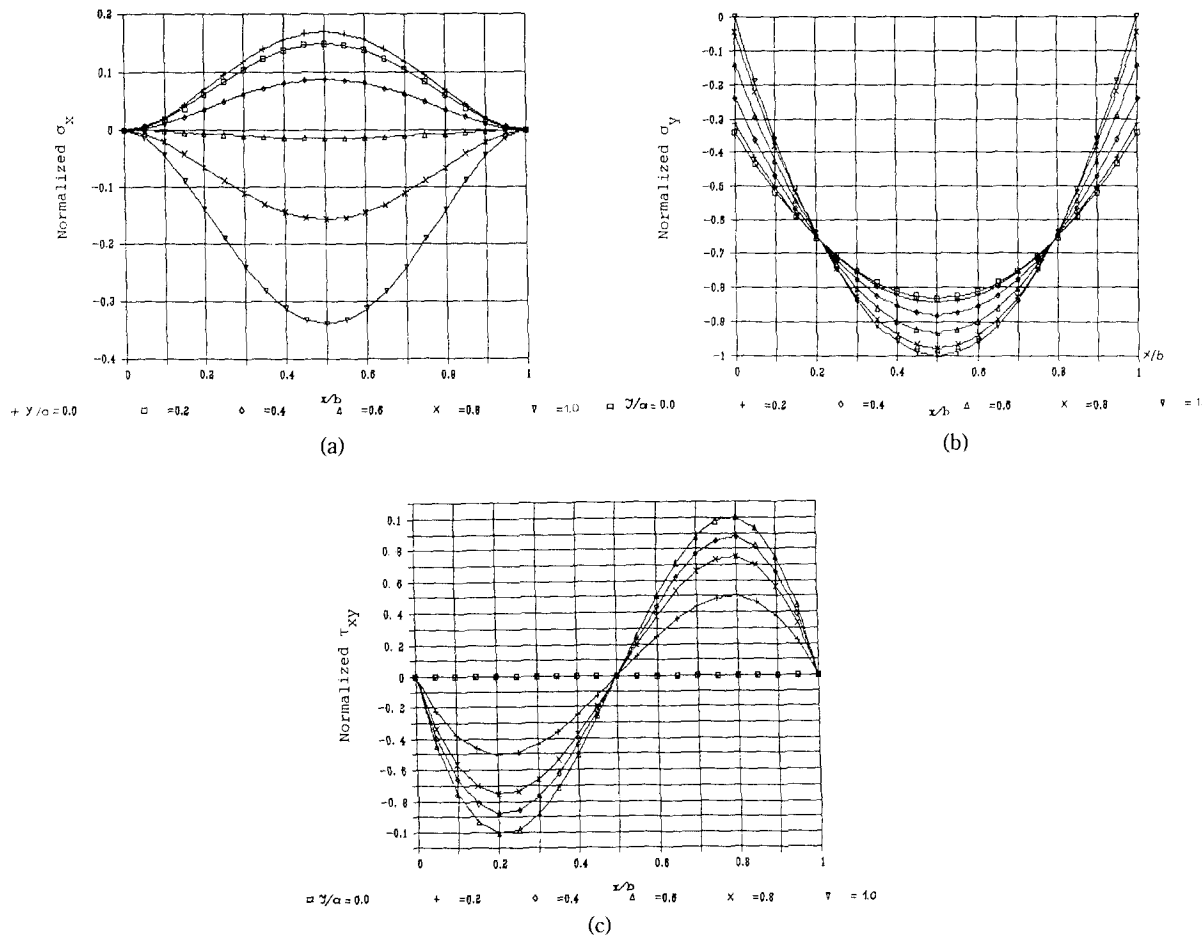

Fig. 14 Stress distribution for the case depicted in Fig. 2: Parabolic load distribution. (a) Distribution of stress σ_x under parabolic loads. (b) Distribution of stress σ_y under parabolic loads. (c) Distribution of stress τ_{xy} under parabolic loads.

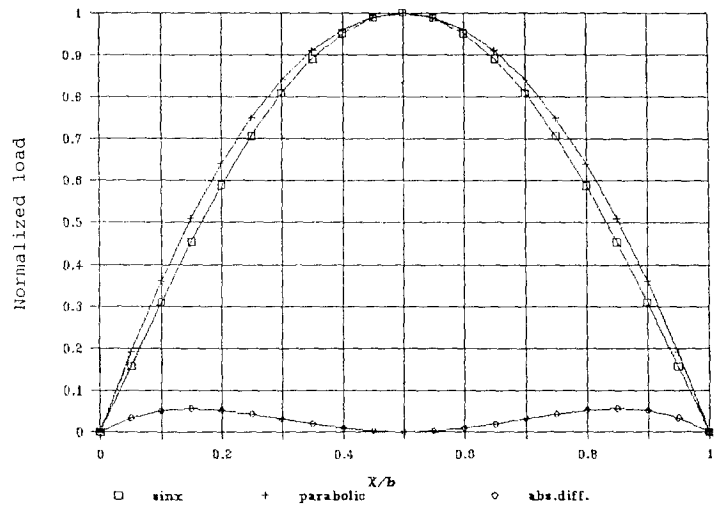

Fig. 15 Normalized difference between parabolic and sinusoidal loadings.

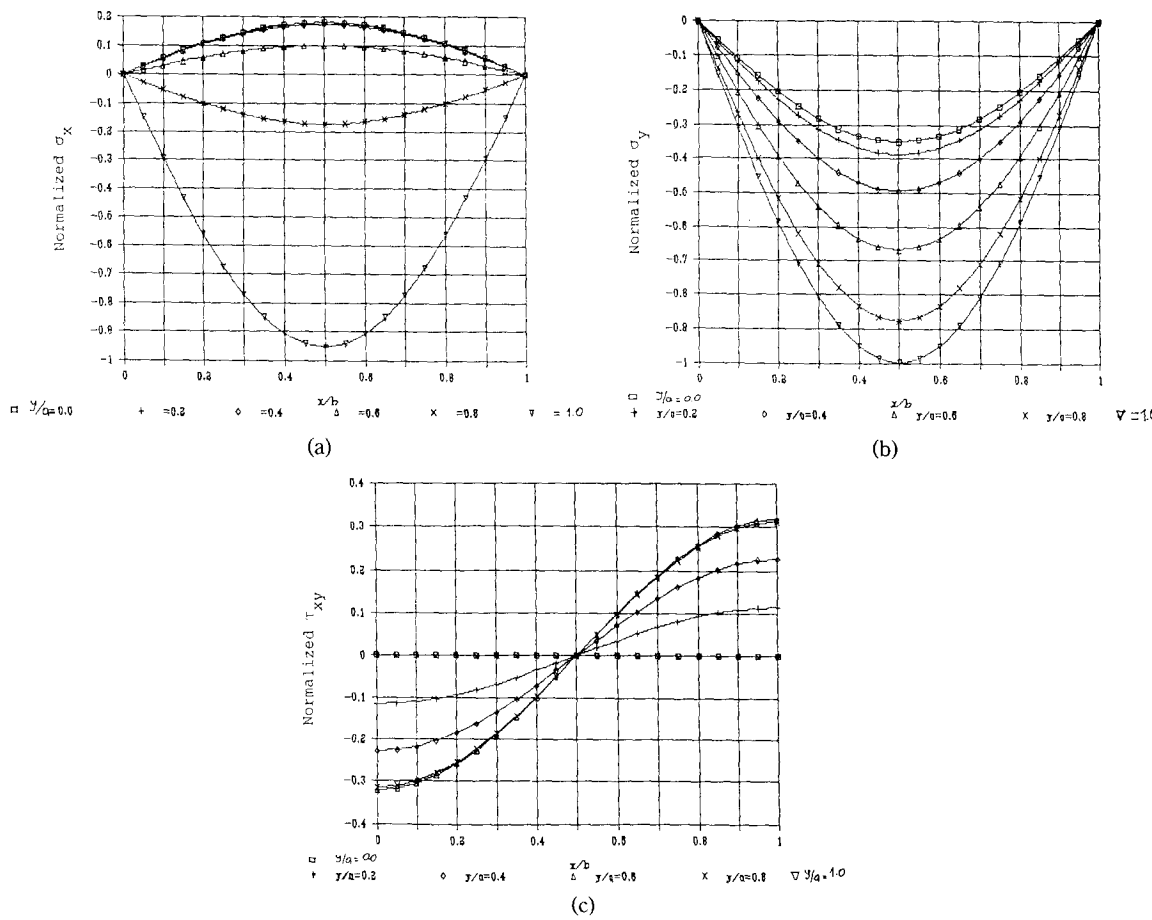

Fig. 16 Stress distribution for the case depicted in Fig. 2: Sinusoidal load distribution. (a) Distribution of stress σ_x under sinusoidal loads. (b) Distribution of stress σ_y under sinusoidal loads. (c) Distribution of stress τ_{xy} under sinusoidal loads.

for $\nu=0$.

The lateral distribution of the stress functions is shown in Fig. 14(a), 14(b), 14(c).

2. Sinusoidal distribution

If the loading distribution in Fig. 13 were sinusoidal there would be a slight difference (<10%), compared with the former loading function, as shown in Fig. 15. The solution assumed in Timoshenko, S. P. and Goodier, J. N. (1987) is:

$$\phi=\sin\frac{\pi x}{l}f(y)$$

$$f(y)=C_1\cosh(\alpha y)+C_2\sinh(\alpha y)+C_3 y\cosh(\alpha y)+C_4 y\sinh(\alpha y) \tag{13}$$

with,

$$\alpha=\frac{\pi}{l}$$

Here again Airy's functions are to be satisfied together with the boundary conditions:

$$y=\mp a\begin{cases}\sigma_y=-S\sin(\alpha x)\\ \tau_{xy}=0\end{cases}\qquad x=\mp b\begin{cases}\sigma_x=0\\ \tau_{xy}=0\end{cases}$$

which results in the following solutions:

$$\sigma_x=\frac{2S\ (\alpha a\cosh\alpha a-\sinh\alpha a)\cosh\alpha y-\alpha y\sinh\alpha y\sinh\alpha a}{\sinh 2\alpha a+2\alpha a}\sin\alpha x$$

$$\sigma_y=-\frac{2S\ (\alpha a\cosh\alpha a+\sinh\alpha a)\cosh\alpha y-\alpha y\sinh\alpha y\sinh\alpha a}{\sinh\alpha a+2\alpha a}\sin\alpha x$$

$$\tau_{xy}=-\frac{2S\ (\alpha a\cosh\alpha a\sinh\alpha y-\alpha y\cosh\alpha y\sinh\alpha a}{\sinh 2\alpha a+2\alpha a}\cos\alpha x$$

The results are given in Figs. 16(a), 16(b), 16(c). Consequently, the difference in results due to the parabolic and sinusoidal distributions is not larger than 10%. However, Fig. 5(c) shows that the boundary condition for shear stress, γ_{xy}, along the vertical edges is not satisfied, and it depends on $\cos(\alpha x)$, with a maximum value along these edges. Also, for the normal stresses, the parabolic distribution yields a better correspondence. Obviously, the trigonometric expansion may consider more terms than one, but then analysis becomes rather complicated.